Abstracts for poster presentations
No. 10 - 18

No. 10

First-principles study on anomalous Hall conductivity in anti-perovskite manganese nitrides Mn_3MN (M= Ni, Cu, Ga, Ge, In, Sn, Ir) with antiferromagnetic structures

Vu Thi Ngoc Huyen[1,2,3], Michi-To Suzuki[4], Kunihiko Yamauchi[2] and Tamio Oguchi[2]

[1] *Graduate School of Engineering Science, Osaka University, Osaka 560-853, Japan*
[2] *Institute of Scientific and Industrial Research, Osaka University, Osaka, Japan*
[3] *National Institute for Materials Science, Osaka, Japan*
[4] *Institute for Materials Research, Tohoku University, Sendai, Japan*
Email: vnhuyen@cmp.sanken.osaka-u.ac.jp

Anomalous Hall (AH) effect was known being able to appear with certain magnetic symmetry in the absence of external magnetic fields [1]. Therefore, this effect can be used for probing spin polarization of electrons in nanoscale systems and memory devices [2]. Conventionally, the AH effect was assumed to be proportional to magnetization leading to no AH conductivity in antiferromagnets with no net magnetization. Nevertheless, the first-principles calculation has predicted the large AH conductivity for the non-collinear antiferromagnet with no net magnetization in Mn_3Ir [3]. Following the finding, non-collinear antiferromagnet Mn_3Ge and Mn_3Sn have been studied to explain the AH effect theoretically and experimentally [2,4–8]. This attractive content of non-collinear antiferromagnetism urges us to search for new materials for spintronic applications. A neutron diffraction experiment reported that some anti-perovskite manganese nitrides Mn_3MN show antiferromagnetism with a triangular magnetic ordering [9]. So Mn_3MN may be candidates for antiferromagnetic spintronic applications. In the present work, we study the structural stability of anti-perovskite manganese nitrides Mn_3MN (M= Ni, Cu, Ga, Ge, In, Sn, Ir) by first-principles calculations. Most of the anti-perovskite manganese nitrides are stable in two non-collinear antiferromagnetic configurations, one kind of which can induce AH effect. The AH conductivity is evaluated by using the Wannier interpolation scheme. In order to understand the microscopic mechanism of the AH conductivity in a non-collinear magnetic system, we discuss the cases of large and small AH conductivity by the cluster multipole theory and electronic band structure analysis. The contribution of the Berry curvature to the AH conductivity is also investigated.

References

[1] S. Naoto Nagaosa, Jairo Sinova, Shigeki Onoda, A. H. Mac- Donald, and N. P. Ong, Rev. Mod. Phys. **82**, 1539 (2010).
[2] S. Nakatsuji, N. Kiyohara1, and T. Higo, Nature **527**, 212 (2015).

[3] H. Chen, Q. Niu, and A. H. MacDonald, Phys. Rev. Lett. **112**, 017205 (2014).
[4] J. Kübler and C. Felser, Europhys. Lett. **108**, 67001 (2014).
[5] N. Kiyohara, T. Tomita, and S. Nakatsuji, Phys. Rev. Applied **5**, 064009 (2016).
[6] A. K. Nayak, J. E. Fischer, Y. Sun, B. Yan, J. Karel, A. C. Komarek, C. Shekhar, N. Kumar, W. Schnelle, J. Kübler, C. Felser, and S. S. P. Parkin, Sci. Adv. **2**, e1501870 (2016).
[7] H. Yang, Y. Sun, Y. Zhang, W.-J. Shi, S. S. P. Parkin, and B. Yan, New J, Phys. **19** 015008 (2017).
[8] M.-T. Suzuki, T. Koretsune, M. Ochi, and R. Arita, Phys. Rev. B **95**, 094406 (2017).
[9] D. Fruchart and E. F. Bertaut, J. Phys. Soc. Jpn. **44**, 3(1978).

No. 11

Observation of impurity band related transitions in high Curie temperature *p*-type ferromagnetic semiconductor (Ga,Fe)Sb

Karumuri Sriharsha[1], Le Duc Anh[1,2], Nguyen Thanh Tu[1] and Masaaki Tanaka[1,3]

[1]*Department of Electrical Engineering and Information Systems, The University of Tokyo*

[2]*Institute of Engineering Innovation, The University of Tokyo*

[3]*Center for Spintronics Research Network (CSRN), The University of Tokyo*

Email: harsha@cryst.t.u-tokyo.ac.jp

Recently, new Fe doped narrow-gap ferromagnetic semiconductors (FMSs) such as p-type (Ga,Fe)Sb [1] and n-type (In,Fe)Sb [2] have shown high-Curie temperature (T_C) ferromagnetism, which is essential for the realization of semiconductor spintronic devices operating at room temperature. Understanding the band structure, especially the position of the Fermi level (E_F), of these materials is strongly required to elucidate the origin of high-T_C ferromagnetism as well as their device applications. In this study, using magnetic circular dichroism (MCD) spectroscopy in an infrared region (photon energy E_{ph} = 0.6 – 1.7 eV), we study the band structure of a series of $(Ga_{1-x},Fe_x)Sb$ samples with various Fe densities x = 2, 6, 10 and 20%. We report evidence for the presence of an impurity band (IB) in the band gap of (Ga,Fe)Sb with the E_F lying inside IB.

The samples examined in this work consist of, from the surface, $(Ga_{1-x},Fe_x)Sb$ (15 nm)/AlSb (300 nm)/AlAs (10nm)/GaAs (50nm), grown on semi-insulating GaAs (001) substrates by molecular beam epitaxy. The transport and magnetic properties of these samples were characterized by Hall measurements and MCD with visible – ultraviolet light (E_{ph} = 1.4 – 6 eV). Samples with x = 6, 10 and 20% show ferromagnetism with T_C = 15, 75 and >320 K, respectively. The MCD spectra in infrared region (E_{ph} = 0.6 - 1.5 eV) of these (Ga,Fe)Sb samples and a reference sample of GaSb thin film, measured at 9 K and 1 T, are shown in Fig. 1. The MCD spectra of the (Ga,Fe)Sb samples show two large peaks, a positive peak E_a lying close to the E_0 transition of GaSb (~0.8 eV) and a new negative peak E_b (~1.4 eV). When x is increased from 2 to 20%, the positions of these two peaks linearly move in opposite directions; E_a shifts to lower energy (from 0.84 eV to 0.54 eV) while E_b shifts to higher energy (from 1.41 eV to 1.58 eV) as shown in Fig 2. The values at x > 6% are smaller than the intrinsic band gap of GaSb (~0.8 eV) indicating the presence of IB in the band gap of $(Ga_{1-x},Fe_x)Sb$ with the E_F lying inside it. As illustrated in Fig 3, E_a likely corresponds to the transition at the Γ point from E_F (in the IB) to the conduction band bottom (Γ_6), while E_b corresponds to the transition at the L point from the valence band (VB) (L_6) to E_F. With increasing x, the IB, which is located close to the VB top at small x, broadens and extends towards the band gap, thereby raising the E_F above the VB top, resulting in the red shift in E_a and the blue shift in E_b. The information of the IB and the position of E_F in (Ga,Fe)Sb revealed in this work is crucial for understanding the magnetic properties and spin device applications of this promising high-T_C FMS.

This work was partly supported by Grants-in-Aid for Scientific Research (No. 17H04922), CREST of JST (No. JPMJCR1777), Yazaki Foundation, and the Spintronics Research Network of Japan (Spin-RNJ).

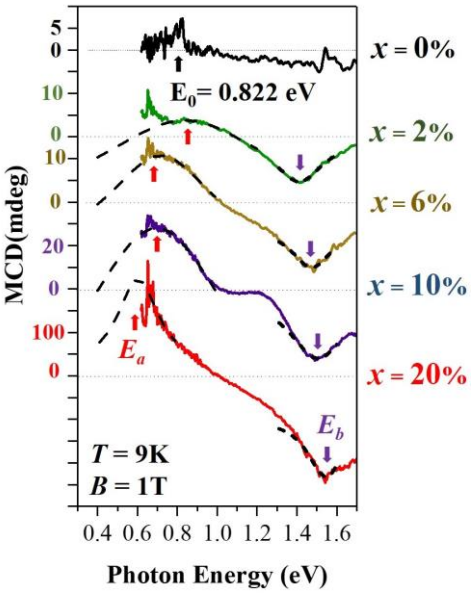

Fig 1. Infrared MCD spectra for the $(Ga_{1-x},Fe_x)Sb$ samples with different Fe densities x (= 0 – 20%).

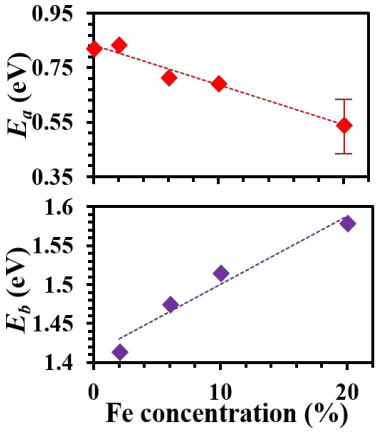

Fig 2. Positions of the E_a and E_b peaks with different Fe density x (= 0 – 20%). For the x = 20% sample, the peak is outside the detectable range, causing the uncertainty.

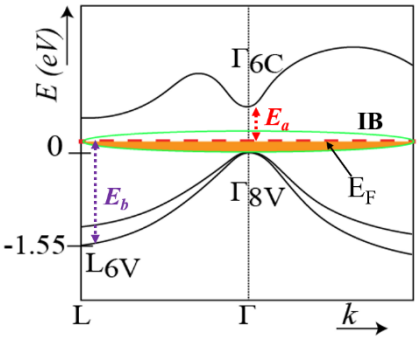

Fig 3. Band structure of (Ga,Fe)Sb showing an impurity band in the band gap and the transitions corresponding to E_a and E_b.

References
[1] N. T. Tu, *et al.*, PRB **92**, 144403 (2015).
[2] N. T. Tu, *et al.*, *APEX* **11** 063005 (2018).

No. 12

Evaluation of temperature-dependent spin Hall angle in CoFeB/MgO/Pt tunneling junctions by using Spin Hall effect tunneling spectroscopy

K. Nakagawara[1], S. Kasai[2], S. Mitani[2], S. Karube[1], M. Kohda[1,3], and J. Nitta[1,3]

[1]*Department of Materials Science, Graduate School of Engineering, Tohoku University, Sendai, Japan*

[2] *National Institute for Materials Science, Tsukuba, Japan*

[3]*Center for Spintronics Research Network, Tohoku University, Sendai, Japan*

Email: knaka@dc.tohoku.ac.jp

Spin Hall effect (SHE) and its inverse effect (i-SHE) are promising ways to generate and to detect spin currents, respectively. The spin Hall angle θ_{SH} is a measure of the conversion efficiency between charge current and spin current. Various methods to evaluate θ_{SH} have been demonstrated [1]-[3]. Recently, SHE tunneling spectroscopy (SHT) [4] has been proposed as an alternative way to evaluate θ_{SH}. In this method, i-SHE signal is obtained via tunneling spin-polarized currents. By using lateral spin valves, spin Hall mechanism (intrinsic and extrinsic spin Hall effect) of Pt has been investigated[5]. In addition to this, the mechanism is also investigated in harmonic measurements[6].

In this study, we experimentally demonstrated the detailed spin-dependent transport mechanism in the spin Hall effect tunneling devices for further understanding the mechanism of spin Hall effect. This method has the potential to measure the temperature-dependent-density of state for evaluation of intrinsic mechanism directly.

Film stack of Ru (8)/Ta (5)/CoFeB (4)/MgO (2)/Pt (7) (thickness in nm) was prepared by magnetron sputtering. The SHT device as shown in Fig.1. One is fabricated by using electron beam lithography and Ar ion milling. CoFeB/MgO junction is patterned into the 4×4 μm^2 square-shaped element. The magneto-transport is measured by using the AC resistance bridge at each temperature. Figure 2 and 3 show an obtained SHT signal, and temperature-dependent spin Hall angle, respectively. The conductivity of this sample is corresponding to the extrinsic mechanism dominant region, but the value is slightly high compared to the spin valve measurement. The further discussion of spin Hall mechanism is undergone.

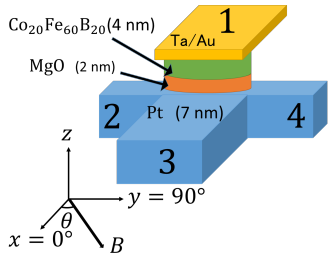

Fig. 1: Sample configuration of SHT device

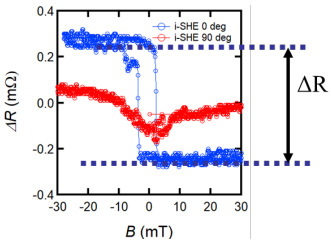

Fig. 2: angular-dependent SHT signal

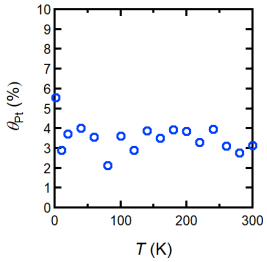

Fig. 3: Temperature-dependent spin Hall angle

References

[1] E. Saitoh *et al.*, Appl. Phys. Lett. **88**, 182509 (2006).
[2] L. Liu *et al.*, Science **336**, 555 (2012).
[3] V. Laurent, *et al.*, Phys. Rev. Lett. **99**, 226604 (2007).
[4] L. Liu *et al.*, Nature Phys. **10**, 561 (2014).
[5] E. Sagasta *et al.*, Phys. Rev. B **94**, 060412 (2016).
[6] G. V. Karnad *et al.*, Phys. Rev. B **97**, 100405 (2018).

No. 13

Study on the magnetization dynamics in magnetic thin films using our proposed measurement technique

Y. Endo[1,2,3], O. Mori[4], Y. Shimada[1,4], S. Yabukami[5], S. Sato[4], and R. Utsumi[4]

[1] *Graduate School of Engineering, Tohoku University, Sendai, Japan*

[2] *Center for Spintronics Research Network (CSRN), Tohoku University, Sendai, Japan*

[3] *Center for Science and Innovation in Spintronics (CSIS), Organization for Advanced Studies, Tohoku University, Sendai, Japan*

[4] *Toei Scientific Industrial Co., Itd., Natori, Japan*

[5] *Graduate School of Biomedical Engineering, Tohoku University, Sendai, Japan*

Email: endo@ecei.tohoku.ac.jp

The magnetization dynamics in magnetic thin films have been studied intensively from both scientific and application points of view. The dynamics are described using phenomelogical Landau-Lifshitz-Gilbert (LLG) equation consisting of both the precession torque of the magnetization and the damping torque [1]. In particular, a Gilbert damping constant (α), which describes the strength of damping torque, is one of the most important parameters to understand the magnetization dynamics. Until now, we proposed a new measurement technique which enables simultaneous evaluation of α and satureation magentostriction (λ_s) by measuring the correlation between ferromagnetic resonance (FMR) frequency (f_r) and the tensile stress, and clarified a correlation between α and λ_s for 50-nm thick Ni-Fe films[2]. Herein, the magnetization dynamics of 10-nm thick Ni-Fe films was investigated by our proposed measurement technique, and the correlation between α and λ_s in these films was discussed.

Figure 1 shows FMR spectra of 10-nm-thick Ni_xFe_{100-x} films either with tensile stress or with tensile stress free. In case of x=78.2 (Fig. 1(a)), each value of FMR frequency with tensile stress ($f_{r\sigma}$) is higher than that of FMR frequency with tensile stress free (f_{r0}) because of uniaxial magnetostrictive anisotropy. The frequency difference ($\Delta f_r = f_{r\sigma} - f_{r0}$) in the external magnetic field (H_{ex}) decreases from +350 to +100 MHz as H_{ex} increases. λ_s evaluated using the $f_{r\sigma}$, f_{r0}, and Δf_r is approximately +1.58 ppm, and is in good agreement with that measured by the optical cantilever method (+3.64 ppm). α is evaluated from f_{r0} and the half-width of the FMR peak with tensile stress free, and is approximately 0.00626. On the other hand, in case of x=84.0 (Fig. 1(b)) every value of $f_{r\sigma}$ is lower than that of f_{r0}. Δf_r in H_{ex} increases from –428 to –34 MHz as H_{ex} increases. λ_s evaluated using the $f_{r\sigma}$, f_{r0}, and Δf_r is approximately –1.25 ppm and agrees well with that measured by the optical cantilever method (–2.91 ppm). α is approximately 0.0107. Furthermore, to clarify the correlation between α and λ_s for 10-nm thick Ni-Fe films, α is plotted in Fig. 2 as a function of λ_s. In the range of positive saturation magnetostriction (λ_s>0), α slightly increases as x decreases, but α increases from 0.00947 to 0.0178 as x increases for negative saturation magnetostriction

(λ_s<0). α reaches a minimum when λ_s is around zero at x = 0.78. This result suggests that the different increment of α depends on positive or negative λ_s. Thus, α and λ_s show a more consistent relation, suggesting that they both originate from spin-orbital coupling [3]. Therefore, these results suggest a correlation between the magnetoelastic properties and α in the Ni_xFe_{100-x} thin films.

This work was supported in part by JSPS KAKENHI Grant Number JP17H03226. This work was also supported in part by CIES collaborative research from CIES, Tohoku University and Advanced Storage Research Consortium (ASRC) in Japan.

References

[1] T. L. Gilbert, IEEE Trans. Magn. **40**, 3443 (2004).
[2] Y. Endo, O. Mori, Y. Shimada, S. Yabukami, S. Sato, and R. Utsumi, Appl. Phys. Lett. **112**, 252403 (2018).
[3] V. Kamberský, Can. J. Phys. **48**, 2906 (1970).

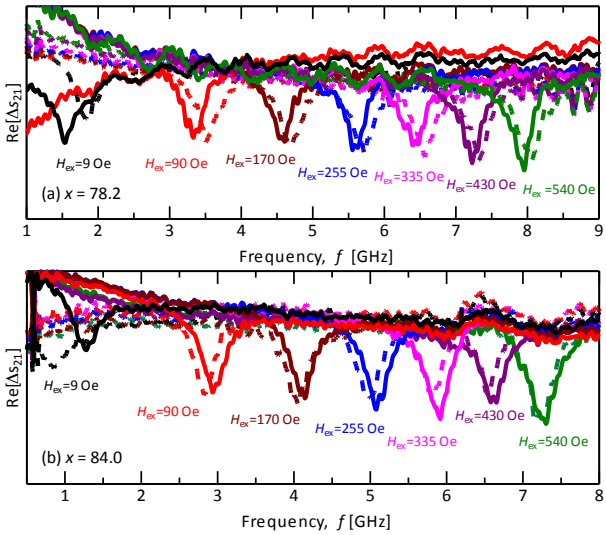

Fig. 1

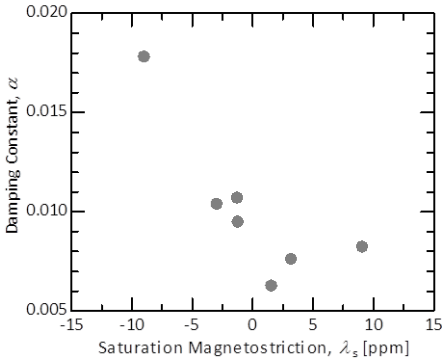

Fig.2

Fig. 1. FMR spectra in various external magnetic fields (H_{ex}) of 10-nm thick Ni_xFe_{100-x} films ((a) x=78.2 and (d) x=84.0) either with tensile stress or with tensile stress free. The dotted line and solid line represent FMR spectra with tensile stress and with tensile stress free, respectively.

Fig. 2. Relationship between the damping constant (α) and the saturation magnetostriction (λ_s) in 10-nm thick Ni_xFe_{100-x} films.

No. 14

Observation of peculiar magnetic anisotropy at the interface of a $La_{0.6}Sr_{0.4}MnO_3/LaAlO_3$ heterostructure

°Le Duc Anh[1,2], Noboru Okamoto[1], Munetoshi Seki[1,3], Hiroshi Tabata[1,3], Masaaki Tanaka[1,3], Shinobu Ohya[1,2,3]

[1]*Department of Electrical Engineering and Information Systems, The University of Tokyo*

[2]*Institute of Engineering Innovation, Graduate School of Engineering, The University of Tokyo*

[3]*Center for Spintronics Research Network, Graduate School of Engineering, The University of Tokyo*

Email: anh@cryst.t.u-tokyo.ac.jp

Control of magnetic anisotropy (MA) is crucial for low-power magnetization reversal in magnetic thin films, which is important for next generation quantum spintronics device applications. From the perspectives of energy efficiency and scalability, gate-voltage control of the MA via modulation of the carrier density and thus, the Fermi level, is highly desirable. For efficient control of MA and for developing materials that are suitable for the MA control, it is necessary to understand the MA of magnetic thin films over a wide energy range; however, there are few studies from this point of view. In ferromagnetic (FM) materials, the MA energy is related to the magnetization-direction dependence of the density of states (DOS) via the spin orbit interaction. Tunneling anisotropic magnetoresistance (TAMR) is a phenomenon observed in tunnel diodes composed of ferromagnetic (FM) layer/ tunnel barrier/ nonmagnetic (NM) electrode. TAMR is defined as the change of the tunnel resistance or conductance dI/dV, which is proportional to the DOS of the electrodes, when rotating the magnetization of the FM layer. Thus, TAMR is useful to understand the magnetic-field direction dependence of the DOS. By measuring TAMR at various bias voltages, one can obtain a high-resolution carrier-energy-resolved map of MA of the FM layer [1].

In this study, using TAMR, we investigate the energy dependence of the MA of the perovskite oxide $La_{0.6}Sr_{0.4}MnO_3$ (LSMO) [2], which is a promising spintronic material due to its half-metallic band structure [3], high Curie temperature (~ 370 K), and colossal magnetoresistance [4]. At the LSMO interface, reconstruction of orbital, charge, and spin configurations occurs due to local structure modifications such as lattice strain and oxygen octahedral rotation, which are only detectable by highly surface-sensitive probes. Understanding these interfacial magnetic properties of LSMO will enable the engineering of the material at an atomic scale, and is thus highly demanded.

The tunnel device structure studied here consists of LSMO (40 unit cell (uc))/ $LaAlO_3$ (LAO, 4 uc) grown on a Nb-doped (0.5 wt%) $SrTiO_3$ (001) (Nb:STO) substrate by molecular beam epitaxy [Fig. 1(a)]. Two-terminal measurements were carried out for 600×700 μm^2 mesa diodes, and the bias polarity was defined so that electrons flow from Nb:STO to LSMO in the positive bias [Fig. 1(b)]. Figure 1(c) shows the change in the tunneling conductance dI/dV with the bias voltage V ranging from –0.5 to +0.5 V applying a magnetic field of 1 T at an angle Φ from the [100] axis in the plane. In addition to the biaxial MA along <100> and the uniaxial MA along [100], which originate from bulk LSMO, we found a peculiar uniaxial MA along the [110], which is attributed to the LSMO/LAO interface. The symmetry axis of this interface MA rotates by 90° at an energy of 0.2 eV below E_F of LSMO, which is attributed to the transition from the e_g band (>–0.2 eV) to the t_{2g} band (<–0.2 eV). These findings hint an efficient way to control the magnetization at the LSMO thin film interfaces, as well as confirm the rich of hidden properties at thin film interfaces that can be revealed only by interface-sensitive probes. This work indicates that the TAMR measurement is a simple but highly sensitive method for characterizing interfacial magnetic properties of MTJs, which is important for developing spintronics devices [5].

This work was supported by Grants-in-Aid for Scientific Research, CREST of JST, and Spin-RNJ.

References:
[1] I. Muneta, T. Kanaki, S. Ohya, and M. Tanaka, Nature Commun. **8**, 15387 (2017).
[2] T. Matou, K. Takeshima, L. D. Anh, M. Seki, H. Tabata, M. Tanaka, and S. Ohya, Appl. Phys. Lett. **110**, 212406 (2017).
[3] J. Park *et al.*, Nature **392**, 794-796 (1998).
[4] A. Urushibara *et al.*, Phys. Rev. B **51**, 14103 (1995).
[5] L. D. Anh, N. Okamoto, M. Seki, H. Tabata, M. Tanaka, and S. Ohya, Sci. Rep. **7**, 8715 (2017).

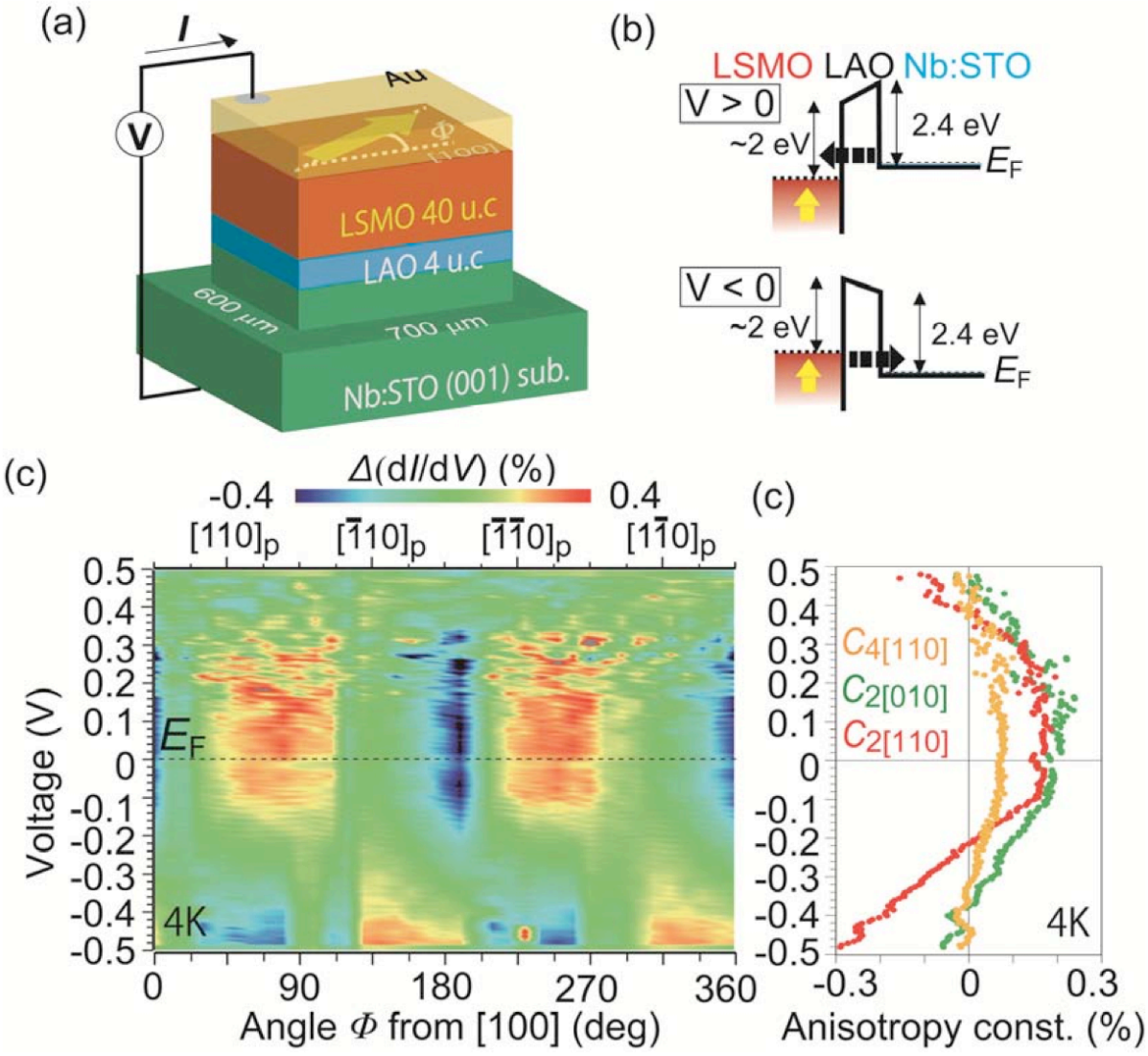

Fig. 1. (a) Device structure used for our measurements. (b) Conduction band (CB) profiles of the LSMO/ LAO/ Nb:STO tunneling diode under positive and negative bias voltages V. The solid and dotted lines represent the top of the CB and the Fermi level E_F. At positive (negative) V, the electrons tunnel from Nb:STO to LSMO (from LSMO to Nb:STO). (c) Color plots of $\Delta(dI/dV) = [dI/dV - \langle dI/dV \rangle_\Phi] / \langle dI/dV \rangle_\Phi \times 100(\%)$ as a function of Φ and V. Here, Φ is the magnetic-field angle from the $[100]_c$ axis in the counter-clockwise direction in the film plane, and $\langle dI/dV \rangle_\Phi$ is defined as averaged dI/dV over Φ at each V. All the data were measured at 4 K [5].

No. 15

Recent Trends in MTJ-Based Nonvolatile FPGA

D. Suzuki[1,3] and T. Hanyu[2,3]

[1] *Frontier Research Institute for Interdisciplinary Sciences, Tohoku Univ., Sendai, Japan*

[2] *Research Institute for Electrical Communication, Tohoku Univ., Sendai, Japan*

[3] *Center for Spintronics Research Network, Tohoku Univ., Sendai, Japan*

Email: daisuke.suzuki.e6@tohoku.ac.jp

In the smart internet of things (IoT) era, VLSI processors from low-end to high-end are indispensable to meet a wide variety of application requirements. A field programmable gate array (FPGA) is an effective way to implement such VLSI processors owing to its reconfigurable architecture. It is also expected that the FPGA is used as a hardware accelerator for brain-inspired computing and its higher energy efficiency compared to software-based method and graphic-processing unit (GPU) based one. However, because a large number of redundant components are required for the FPGA, standby power dissipation is a critical issue for the conventional SRAM-based FPGA. Therefore, like sensor node applications that operate under limited electricity such as an installed maintenance-free battery or energy harvesting is not suitable for the SRAM-based FPGA.

A nonvolatile FPGA (NV-FPGA), wherein all the data are stored in nonvolatile devices is one promising solution for the standby power problem. Because the circuit information is remained without power supply, standby power consumption is completely eliminated by utilizing power gating technique where power supply of idle circuit blocks are temporally cut off. Among several emerging nonvolatile devices, a magnetic tunnel junction (MTJ) device is a viable candidate given its 3-dimensional stacking capability, CMOS compatibility, and virtually unlimited endurance.

In this presentation, recent research trends in MTJ-based NV-FPGA [1-4] are presented. Especially, the advancements of a lookup table (LUT) circuit which is key component of the FPGA are presented.

References

[1] D. Suzuki et al., Symp. VLSI Circuits Dig. Tech. Papers, 172 (2015).
[2] D. Suzuki, et al., IEEE Trans. Magn. **50**, 3402104 (2014).
[3] D. Suzuki, et al., IET Electronics Lett. **53**, 456 (2017).
[4] D. Suzuki and T. Hanyu, Jpn. J. Appl. Phys. **57**, 04FE09 (2018).

No. 16

Anomalous Magnetic, Dielectric, and Optic Properties in Strained and Relaxed Rare-earth Iron Garnet Thin Films

Hiroyasu Yamahara[1], Sarker Md Shamim[1], Akihiro Katougi[1], Ryota Kikuchi[1], Munetoshi Seki[1], and Hitoshi Tabata[1]

[1] *University of Tokyo*, *Tokyo, Japan*

Email: yamahara@bioxide.t.u-tokyo.ac.jp

Rare-earth iron garnets (RIGs) are ferrimagnetic insulators whose chemical formula is $R_3Fe_5O_{12}$ (R : rare-earth elements). They have been commercially available for optical devices such as optical isolators since they show large magneto-optical effect. Among various RIGs, $Y_3Fe_5O_{12}$ (YIG) is widely studied for spinwave applications since the intrinsic Gilbert damping constant is exceptionally low as $\alpha = 10^{-5}$ in bulk. In this research, magnetic, dielectric, and optic properties of crystalline strained and relaxed RIG films are studied. YIG grown on $Gd_3Ga_5O_{12}$ (GGG) substrates has shape anisotropy with in-plane easy axis, while YIG on $Y_3Al_5O_{12}$ (YAG) are reported to shows strain-tunable magneto-crystalline anisotropy due to the strain-induced tetragonal distortion [1]. On the other hand, perpendicular magnetic anisotropy is reported in strained $Tm_3Fe_5O_{12}$ (TmIG) [2] and $Sm_3Fe_5O_{12}$ (SmIG) [3] thin films. When there is a lattice mismatch between RIG films and substrates, the crystal structure is epitaxially strained, therefore tetragonal structure is observed in the vicinity of interface. As the film thickness increase, misfit dislocation occurs at critical thickness t_c and lattice relaxation occurs. Around the surface, relaxed cubic structure is observed. At the vicinity of t_c, strain and relaxation co-exist, therefore strain-gradient structure is grown as illustrated in Figure 1. In the strain-gradient region, the asymmetric crystal structure is expected to generate electrical polarization known as flexoelectricity [4]. Since there are both magnetic moments and electrical polarization in the strain-gradient structure, multiferroic behaviors and magneto-electric correlation (ME-effect) are expected, which is useful for future application on spintronics devices. In this research, magnetic, dielectric and optical properties of SmIG thin films deposited on GGG substrates are discussed. The lattice mismatch between SmIG and GGG is 1.2%, so that the critical thickness t_c, where misfit dislocation occurs, is estimated to be 66 nm. When the thickness of SmIG is thicker than t_c, strain-gradient structure is expected between coherently strained tetragonal and relaxed cubic phases. SmIG films with various thickness are grown by pulsed laser deposition technique (PLD). The epitaxial relationship between films and substrates are confirmed by reciprocal space mapping (RSM) of X-ray diffraction (XRD). The magnetic property measurements are carried out by magnetic circular dichroism (MCD). In order to measure dielectric properties of SmIG films, interdigital electrodes (IDE) with 10 μm width and space are fabricated by photolithography and metal sputtering. Spectroscopic ellipsometry is measured for

optical property analysis.

Figure 2(a) shows thickness dependence of magnetic coercive field measured by MCD. When the thickness of SmIG film is around critical thickness, the magnetic coercivity shows maximum, which is because defects work as pinning sites of domain wall. Figure 2(b) shows thickness dependence of dielectric constant measured by using IDE. The dielectric constants are characterized from capacitance measured by impedance spectroscopy. In order to calibrate the effect of electrodes geometries and film thickness, calculation model reported by Farnell is applied [5]. As shown in Figure 2(b), dielectric constants shows maximum around critical thickness. The refractive indexes of SmIG films are also characterized by spectroscopic ellipsometry. We observe lower shift of light absorption edge for SmIG films that thickness is around critical thickness. These anomalous behaviors relate to dislocations and strain-gradient structures.

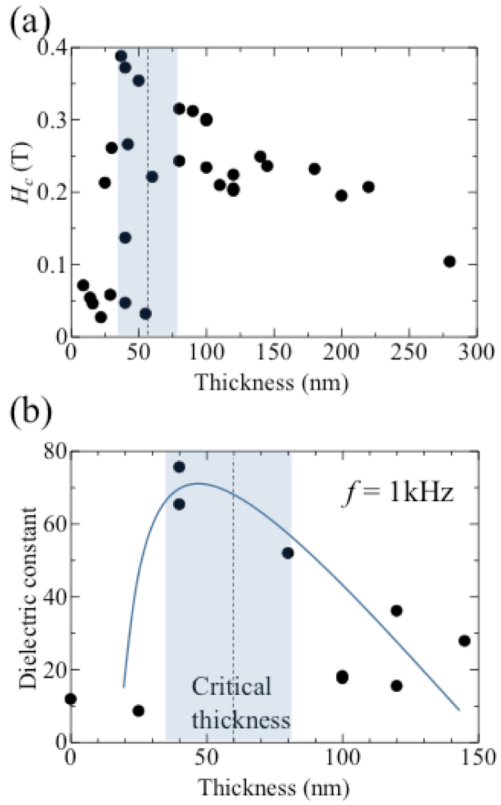

Figure 1. Schematic illustration of strained-tetragonal, strain-gradient, and relaxed cubic structures.

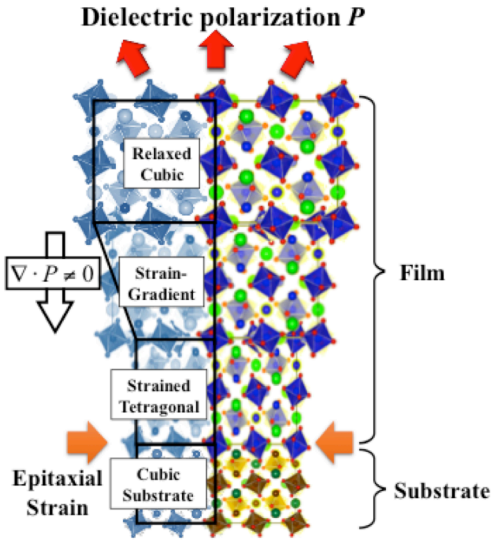

Figure 2. (a) Thickness dependence of coercive field measured by MCD. (b) Thickness dependence of dielectric constant measured by using interdigital electrodes.

References

[1] H. Wang et al., Phys. Rev. B, 89 134404 (2014).
[2] C. Tang et al., Phys. Rev. B, 94 140403 (2016).
[3] H. Yamahara et al., J. Mag. Mag. Mater., 323 3143 (2011).
[4] D. Lee et al., Phys. Rev. Lett. 107 057602 (2011).
[5] G. W. Farnell et al., IEEE. Trans. Sonics. Ultrason., SU-17, 188 (1970).

No. 17

Physical Implementation of Neuromorphic System

M. S. Sarker[1], H. Yamahara[1], M. Seki[1,2], Y. Hotta[3], and H. Tabata[1,2]

[1] *Department of Electrical Engineering and Information Systems, Graduate School of Engineering, University of Tokyo, Japan*

[2] *CSRN, Graduate School of Engineering, University of Tokyo*

[2] *Department of Electrical Materials and Engineering, University of Hyogo*

Email: yamahara@bioxide.t.u-tokyo.ac.jp

Neuromorphic system is an interdisciplinary research platform which incorporates the knowledge of biology, physics, mathematics, computer science and electronic engineering to design an artificial neural system. The artificial neural system is widely applied for vision system, head to eye system, auditory processors and autonomous robots, whose physical architecture and design principles are based on those of biological nervous system [1]. The accurate understanding of the morphology of individual neuron, its circuit application, overall architecture, incorporating the adaptability towards any environmental change and finally the learning and developments are the key aspects of the successful implementation of neuromorphic system. The hardware level implementation of the neuromorphic computing can be realized by oxide based memristor [2], threshold switch and transistor [3]. The fundamental part of the neuromorphic system design is to implement a system that can mimic the function of an individual neuron. Hotta et al. proposed a system named neuron like signal transducer (NST) based on stochastic resonance (SR) which can replicate the function of neuron [4]. In their report they used stochastic resonance between the weak neuron like signal and another signal with fixed amplitude, but wide range of frequency called Gaussian White Noise (GWN) to amplify and detect the weak biological signal. They used a comparator with a fixed threshold voltage in such a way that when the amplified signal crosses a predefined threshold then it will produce a neuron like spike signal. This predefined threshold of this NST limits it boundary to act like the biological neuron because predefined threshold makes its behavior more deterministic and can not react against the unpredictable and abrupt environmental change. To overcome this limitation a stochastically excitable threshold unit model has been reported [5] which uses multiple attractor. This is purely a simulation model which can mimic the stereopsis and binocular rivalry in the human visual cortex. The first target of this research is to implement this SR model of the attractor switching device using chip and characterize this neural system. The second stage is to adapt the multifunctional oxide-based memristor or active devices on the chip to design a complete neuromorphic system.

References

[1] Boddhu, S. K., Gallagher J. C., Appl. Comp. Intel. and Soft Computing, 1–21, 2012. [2] Maan, A. K.; Jayadevi, D. A.; James, A. P, IEEE Trans. on Neural Networks and Learning Systems. 99, 2016. [3] Zhou Y., Ramanathan S., Proc. of the IEEE. 103, 1289–1310, 2015. [4] Y. Hotta et al., Appl. Phys. Lett., 1, 088002, 2008. [5] N. Asakawa, Y. Hotta, T. Kanki, T.kawai, Phys. Rev. E 79, 021902, 2009.

No. 18

Thermal effect in magnetization dynamics induced by electric-field in a magnetic tunnel junction

S. Kanai,[1-3] Y. Nakatani,[4] F. Matsukura,[1-3,5,7] and H. Ohno[1-3,5-6]

[1]Laboratory for Nanoelectronics and Spintronics, Research Institute of Electrical Communication, Tohoku University, *Sendai, Japan*

[2]Center for Spintronics Integrated Systems, Tohoku University, *Sendai, Japan*

[3]Center for Spintronics Research Network, Tohoku University, *Sendai, Japan*

[4]University of Electro-Communications, *Tokyo, Japan*

[5]Center for Innovative Integrated Electronic Systems, Tohoku University, *Sendai, Japan*

[6]Center for Science and Innovation in Spintronics (Core Research Cluster), Tohoku University, *Sendai, Japan*

[7]WPI-Advanced Institute for Materials Research, Tohoku University, *Sendai, Japan*

Email: sct273@riec.tohoku.ac.jp

Electric-field induced magnetization switching was demonstrated in nanoscale magnetic tunnel junctions (MTJs). While clear oscillations in the switching probability were observed [1, 2], their amplitude decays within 5 periods, suggesting 10 times larger thermal agitation in magnetization dynamics expected from nucleation volume and damping constant. In this work, we measure magnetization dynamics in an MTJ by measuring transmitted voltage to elucidate the origin of this inconsistency.

An 80-nm-diameter MTJ with CoFeB (0.9 nm)/MgO/CoFeB (1.8 nm) is fabricated by sputtering and electron beam lithography. The CoFeB layers have perpendicular easy axis, and the 1.8-nm (0.9-nm) CoFeB layer is free (reference) layer. We induce the free layer magnetization precession about the in-plane component of external magnetic field by applying voltage pulses with ns duration. The magnetization dynamics is monitored as the transmitted voltage using high-speed oscilloscope, which reflects the perpendicular magnetization component in the free layer through the tunnel magnetoresistance effect.

The single-shot measured magnetization precession manifests itself as a clear oscillation with a 2 ns oscillatory period in the transmitted voltage. The amplitude of oscillation does not show significant decay up to ~6 periods, while the phase of the oscillation shifts randomly with time. It is clarified that oscillation frequency depends on its amplitude. Taking this phase-amplitude coupling into account, the decays of the averaged oscillation in transmitted voltage and switching probability within ~5 periods [1,2] are explained by thermal effect expected from nucleation volume and damping constant.

This work was supported in part by R&D Project for ICT Key Technology of MEXT, and the Cooperative Research Project of RIEC, Tohoku University.

References

[1] Y. Shiota *et al*., Nature Mat. **11**, 39 (2012).
[2] S. Kanai *et al*., Appl. Phys. Lett. **101**, 122403 (2012).